JGR Solid Earth

RESEARCH ARTICLE
10.1029/2021JB023643

Velocity and Anisotropic Structure of the Uppermost Mantle Beneath Central America and Northwestern South America From Pn Tomography

Yan Lü[1,2,3], Juan Li[1,2,3], Yuhui He[1,2,3], Lian-Feng Zhao[1,2,3], and Jinhai Zhang[1,2,3]

[1]Key Laboratory of Earth and Planetary Physics, Institute of Geology and Geophysics, Chinese Academy of Sciences, Beijing, China, [2]University of Chinese Academy of Sciences, Beijing, China, [3]Heilongjiang Mohe Observatory of Geophysics, Institute of Geology and Geophysics, Chinese Academy of Sciences, Beijing, China

Key Points:

- The first comprehensive uppermost mantle Pn velocity and anisotropy model in Central America and northwestern South America was presented
- Separate hot mantle material upwelling is observed beneath the back-arc volcano in Nicaragua
- The patterns of Pn velocity and anisotropy are discontinuous near the Caldas Tear

Supporting Information:

Supporting Information may be found in the online version of this article.

Correspondence to:

Y. Lü,
lvyan@mail.iggcas.ac.cn

Citation:

Lü, Y., Li, J., He, Y., Zhao, L.-F., & Zhang, J. (2022). Velocity and anisotropic structure of the uppermost mantle beneath Central America and northwestern South America from Pn tomography. *Journal of Geophysical Research: Solid Earth*, *127*, e2021JB023643. https://doi.org/10.1029/2021JB023643

Received 14 NOV 2021
Accepted 17 MAR 2022

Abstract We constructed the first Pn velocity and anisotropy model of the uppermost mantle in Central America and northwestern South America using the Pn tomography method and new ISC-EHB data. Significantly low Pn velocities and arc-parallel anisotropic structures are observed beneath the volcanic arc in Central America. The separate, low Pn velocity beneath the back-arc volcano in Nicaragua shows that the hot material upwelling in the uppermost mantle beneath this volcano is likely separated from the main volcanic arc. The stable Caribbean Plate is characterized by high Pn velocities. The southward subduction and dehydration of the Caribbean Plate seem to be potential causes of the low Pn velocities in eastern Panama. Based on our Pn velocity, anisotropy and previous geological observations, we suggest a dynamic model of the Colombia-Ecuador region including mantle flow and magmatic gap: there is arc-parallel anisotropy in the uppermost mantle beneath the Colombia-Ecuador volcanic arc, arc-perpendicular mantle flow in the deeper mantle beneath the subducted plate, and a magmatic gap near the Caldas Tear.

Plain Language Summary The multiplate collision system in Central America and northwestern South America produced the complex tectonic structure of this region. We obtained the seismic velocity and anisotropy models of the uppermost mantle in this region with a reliable tomography method and new seismic data. The results reveal significantly low Pn velocities and arc-parallel anisotropic structures beneath the volcanic arc in Central America and the Colombia-Ecuador area. The separate, low Pn velocity beneath the back-arc volcano in Nicaragua shows that the hot upwelling in the uppermost mantle beneath this volcano may be separate from the main volcanic arc. Low velocities are also observed beneath the Colombia-Ecuador volcanic arc, and the Pn velocity and anisotropy pattern are discontinuous on the two sides of the Caldas Tear. The new Pn velocity and anisotropy models provide additional seismic information about the plate convergence process and establish new constraints on the plate subduction and upwelling of hot mantle material.

1. Introduction

Central America and northwestern South America are areas where the Nazca and Cocos plates converge and collide with the South American and Caribbean plates. These areas have complex plate tectonics, frequent volcanic earthquakes, and are important for investigating the plate dynamic processes (Hey, 1977; Lonsdale, 2005; Pennington, 1981; Taboada et al., 2000; van Benthem et al., 2013; Figure 1). By means of tomography and other methods, previous studies have observed the subduction of the Cocos Plate under the North American Plate and the Caribbean Plate on a large scale, and plate dehydration caused the zonal volcanic distribution in Central America (Amaru, 2007; Bijwaard et al., 1998; Harmon et al., 2013; Li et al., 2008). The subduction of the Nazca Plate beneath the South American Plate and the upwelling of mantle thermal material associated with plate dehydration have also been observed (van Benthem et al., 2013; Vargas and Mann, 2013). In Panama, predecessors used seismicity to outline the subducting segment of the Caribbean Plate (Camacho et al., 2010). In northern South America, the ancient Caribbean Plate, with high seismic velocity and subducting southward, and the Farallon Plate have been observed in the mantle (Bezada et al., 2010; Bijwaard et al., 1998; Harris et al., 2018; Miller et al., 2009; van Benthem et al., 2013; van der Hilst et al., 1997). The westward movement of mantle thermal material flow from the eastern Lesser Antilles subduction zone is thought to have affected the uppermost mantle in northern South America (Masy et al., 2011; Miller et al., 2009). However, due to data or method limitations, the imaging resolution of previous studies was insufficient to accurately answer some remaining questions. For

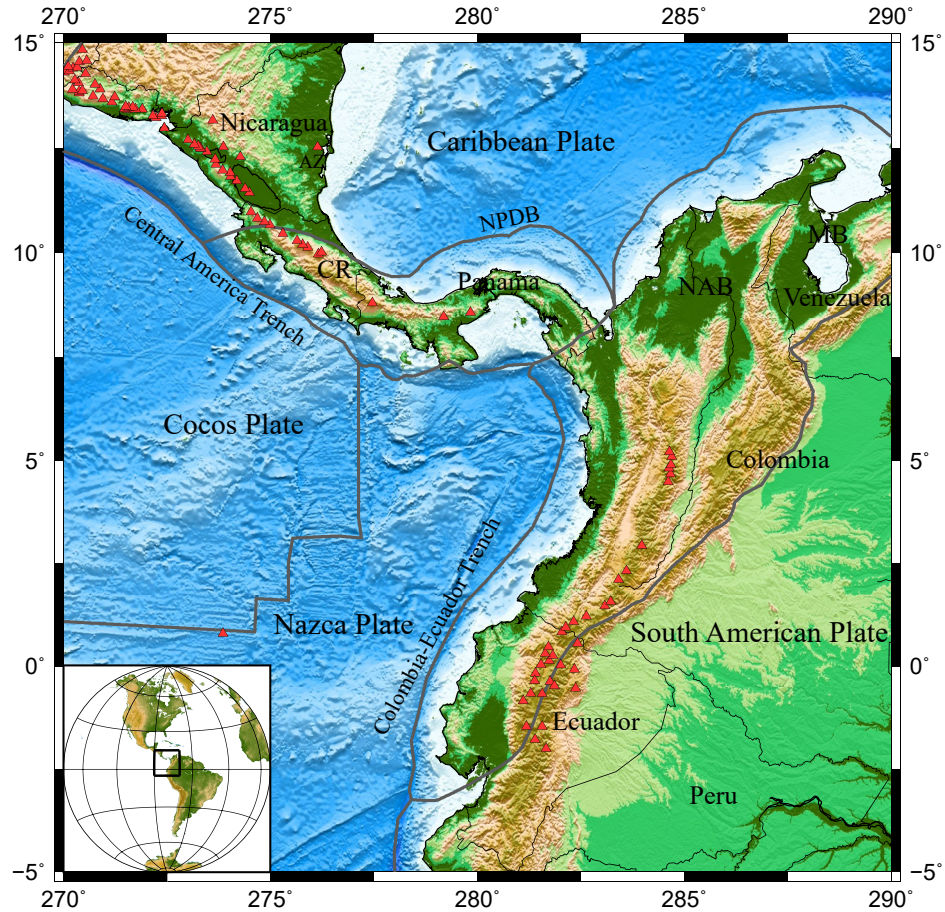

Figure 1. Map of areas in Central America and northwestern South America. The triangles represent Quaternary volcanoes. The gray lines denote major tectonic boundaries. AZ, Azul Volcano; CR, Costa Rica; MB, Maracaibo Block; NAB, North Andes Block; NPDB, North Panama Deformed Belt.

example, what is the relationship between the Panamanian volcanic gap, the eastward subduction of the Cocos Plate and the southward subduction of the Caribbean plate? What is the structure of the upper mantle beneath the back-arc volcano in Nicaragua? Do the velocity and anisotropic structures differ between the north and south sides of the Caldas Tear zone? These scientific problems need to be further addressed by more detailed imaging results.

In addition, seismic anisotropy is an important constraint for studying the deep dynamic process of the earth and can provide the strain characteristics retained by the present or the last major dynamic process in the interior of the earth (Becker et al., 2012; Buehler & Shearer, 2017; Long & Becker, 2010; Menke, 2015; Sandvol et al., 1994; Zhao et al., 2016). Previous anisotropy studies in this area are obtained dominantly from the shear wave splitting analysis (Abt et al., 2010; Growdon et al., 2009; Idarraga-Garcia et al., 2016; Lynner & Long, 2014; Piñero-Feliciangeli & Kendall, 2008; Porritt et al., 2014; Russo & Silver, 1994). The fast direction of shear waves in Central America is generally parallel to the plate collision boundary (Abt et al., 2010; Porritt et al., 2014). In northwestern South America, the results of shear wave anisotropy also provide constraints for the deep structure of this region (Idarraga-Garcia et al., 2016; Porritt et al., 2014; Russo & Silver, 1994). However, the shear wave splitting method can obtain results only below the stations, and thus there is a lack of anisotropic results in regions with limited or no stations. Moreover, this type of measurements reflects the integral of anisotropic structures over a wide range of depths. Thus, anisotropic structures sensitive to specific depths, combined with velocity imaging, are needed to help us further reveal the characteristics of deep structures and dynamic processes.

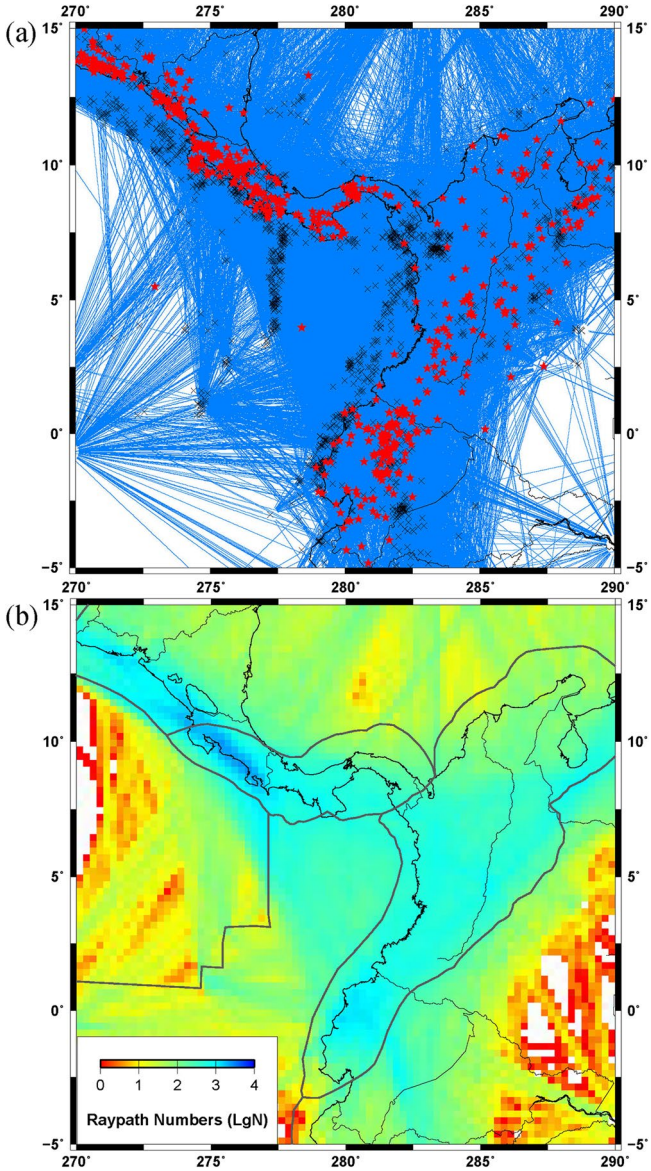

Figure 2. (a) The Pn raypaths of the study area. The red stars represent stations. The black crosses represent events. (b) Raypath numbers in each cell with size of 15′ × 15′.

The Pn velocity and anisotropy tomography method can provide the lateral velocity and anisotropic structure in the uppermost mantle (Hearn, 1996; Lü et al., 2017). The Pn velocity variations reflect the variations in the temperature, composition, and volatile content of the uppermost mantle; Pn anisotropy is related to the preferred orientation of the minerals, reflecting the stress state in the uppermost mantle and the mantle dynamic process (Buehler & Shearer, 2010; Hearn, 1999; Karato & Jung, 1998). Since Pn waves propagate transversely in the uppermost mantle, the ray density is high, and the lateral inversion resolution is greater (Buehler & Shearer, 2010; Hearn & Ni, 1994; Lei et al., 2014; Li & Song, 2018; Liang et al., 2004; Lü et al., 2017; Pei et al., 2007, 2011). Recent studies have shown that Pn imaging results can obtain finer structures, which provide new constraints for deep structures and dynamic processes (Lü et al., 2017, 2019). In this study, we collect the ISC-EHB data in Central America and northwestern South America. With the new data set, we are able to obtain high-resolution Pn velocity and anisotropy imaging, which are sufficient to address finer uppermost mantle structures, and provide new seismological constraints for the complex plate dynamics of the study area.

2. Data and Method

2.1. Data

The study area is defined between 5°S and 15°N and between 270°E and 290°E (Figure 2a). The Pn data we used are from the latest ISC-EHB bulletin (1964–2017) (Engdahl et al., 2020). The following standards were used on the Pn data selection to ensure the inversion quality: epicenter distances between 2° and 12°, every seismic event has picks associated to at least four stations, and every station recorded at least four Pn data; traveltime residuals were no more than 5 s. In total, 67,857 Pn data from 3290 events recorded by 1,484 stations between 15°S and 25°N and between 260°E and 300°E were used.

2.2. Method

The anisotropic Pn tomography method was developed by Hearn (1996, 1999). The layer of uppermost mantle is divided into two-dimensional cells in which the velocity and anisotropy items are inverted. We used the cell size of 15′ × 15′ with ray numbers in each cell that were more than 30 in most of our discussed areas (Figure 2b). As pointed out by previous studies, the addition of anisotropy in Pn tomography not only provides the anisotropic structure, but also improves the velocity results (He & Lü, 2021; Hearn, 1999; Lü et al., 2019). Therefore, we applied the anisotropic Pn tomography method and do not present the isotropic inversion result in this study.

The equation of the anisotropic Pn traveltime residuals is described by:

$$T_{ij} - \Delta T_{ij} = a_i + b_j + \sum_k d_{ijk} \cdot (S_k + A_k \cos 2\phi_{ijk} + B_k \sin 2\phi_{ijk}) \quad (1)$$

where T_{ij} is the travel time residual for event j at station i; ΔT_{ij} is the Moho depth correction for ray ij; a_i is the static delay for station i; b_j is the static delay for event j; d_{ijk} is the travel distance of ray ij in mantle cell k; S_k is the slowness perturbation for cell k; A_k and B_k are the anisotropy coefficients for cell k; ϕ_{ijk} is the back azimuth angle of ray ij in cell k. The anisotropy magnitude is given by $\sqrt{A_k^2 + B_k^2}$, and the direction of

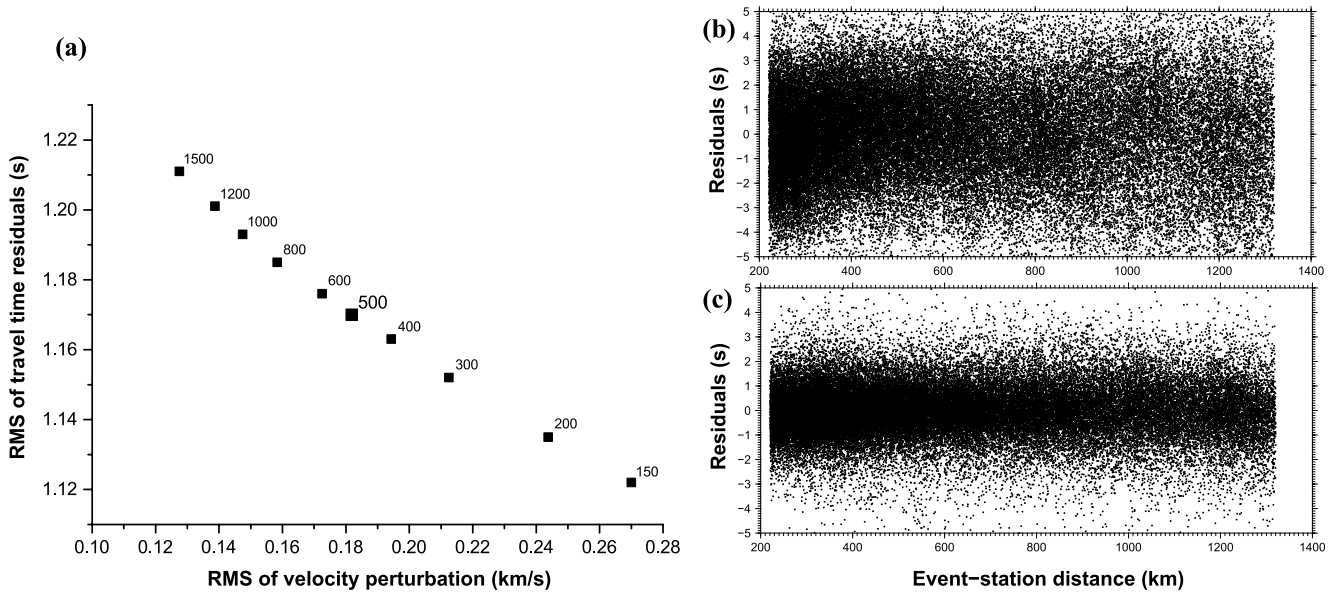

Figure 3. (a) Trade-off between traveltime residuals and velocity perturbations with different damping values. The residual distribution (b) before and (c) after inversion.

the fastest wave propagation is given by $90^{\circ} + \frac{1}{2} arctan \frac{B_k}{A_k}$. The equations were solved by the LSQR method (Paige & Saunders, 1982). Two same damping constants were used to the velocity and anisotropy items (Hearn, 1999; Lü et al., 2017; Pei et al., 2007). The damping constants were chosen considering the trade-off between traveltime residuals and velocity perturbations (Figure 3a). Two hundred inversion iterations were performed with damping value of 500 for the velocity and anisotropy items. The station and event delays are not damped. The root mean square of travel time residuals decreased from (Figure 3b) 2.0 s to (Figure 3c) 1.2 s after inversion.

The station and event delay items were used to absorb the traveltime delays due to the crustal model, event location and event time errors. The station delays are mainly related to the differences between the initial crustal model and the real crust. Positive station delays indicate a thicker crust or lower velocity of crust. The event delays also reflect the event location and event time errors and are generally larger than the station items (Figure 4b).

We applied the checkerboard tests to make clear the anomaly sizes that can be imaged reliably. The average amplitudes ($max\Delta v/\sqrt{2}$) of the sinusoidal input velocity and anisotropy were 0.3 km/s. The checkerboard test results showed that in the areas with high ray densities (Figure 2b), the resolution of velocity can reach 1.5° × 1.5° or better and the resolution of anisotropy can reach 2.0° × 2.0° (Figure 5). The resolutions of the uppermost mantle in most of our discussed areas are better than those of previous studies and are sufficient to present much finer structures. The southwestern and southeastern parts of the study area have relatively low resolution, so we only discuss the results of the areas with better resolution.

3. Results

3.1. Pn Velocity

A strong Pn low-velocity region has been observed in Central America in the northwestern part of the study area, and the banded low-velocity region corresponds to the surface volcanic zone (Figure 6 and Table S1). There is a small-scale independent Pn low-velocity structure near Azul Volcano in eastern Nicaragua. In Panama, the Pn low-velocity zone ends in central Panama (~280°E), but a small-scale low-velocity anomaly has also been observed in eastern Panama. In the Colombian-Ecuador region, a banded strong low-velocity zone corresponding to the surface volcanic zone is observed, and this low-velocity zone is discontinuous at the Caldas Tear. Weak low

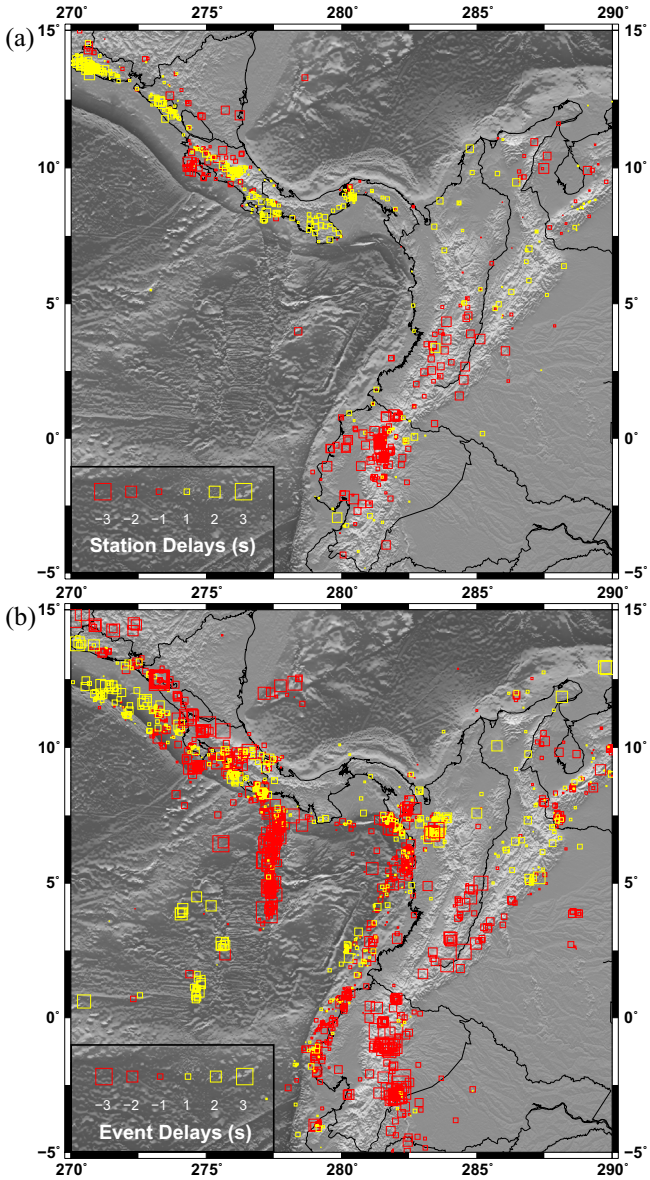

Figure 4. (a) Station and (b) event delays in the study area. Sizes of the squares are proportional to the delay.

velocities have also been observed in northern and northeastern Colombia. The Caribbean plate mainly presents high Pn velocities as well as in western Venezuela.

3.2. Pn Anisotropy

Figure 7 shows the Pn anisotropic structure of the study area. We mainly focus on the anisotropy results in the relatively dense regions of ray distribution. The Pn anisotropy of the NW-SE fast wave direction parallel to the plate collision boundary is observed under the volcanic arc in Central America (region A). In northern Colombia, the direction of Pn anisotropy is very complex (region B). The NNE-SSW Pn anisotropy parallel to the plate collision boundary is also observed under the volcanic zone in the Colombia-Ecuador region (region C).

4. Discussion

4.1. Central America

In Central America in the northwestern part of the study area, the most prominent feature of the Pn velocity structure is the strong low-velocity structure corresponding to the distribution of the volcanoes. The lowest anomalies are larger than 5%, which indicates the high temperature or partial melting structure in the uppermost mantle caused by subduction dehydration of the Cocos Plate. This low-velocity band has been observed in various tomographic studies (Amaru, 2007; Harmon et al., 2013; Li et al., 2008; van Benthem et al., 2013). However, beneath the back-arc volcano (Azul Volcano; Brasse et al., 2015; Carr et al., 2003) in eastern Nicaragua, previous imaging results show large-scale low-velocity structures in the upper mantle (~100 km depth) that are continuous with low velocities under the volcanic arc (Amaru, 2007; Li et al., 2008; van Benthem et al., 2013). Some tomography efforts using local seismicity have not been able to reach this area (Syracuse et al., 2008; Van Avendonk et al., 2011). Here, we have observed an independent small-scale low-velocity zone of the uppermost mantle (<30 km beneath the Moho) beneath the Azul Volcano area, which is not continuous with the low-velocity zone under the volcanic arc. Due to the high resolution in the uppermost mantle, this result is reliable. Furthermore, this methodology has been successfully applied to reveal independent small-scale low-velocity structures under intraplate volcanoes in northeastern China (Lü et al., 2019), which have been further verified by ambient noise tomography with dense stations (Fan et al., 2021). The results of the low-velocity structure indicate that temperatures beneath the Azul Volcano are still high in the uppermost mantle, and the thermal anomaly caused by upwelling hot material are kept till now. Based on the tectonic evolution of the study area, we argue that this mantle thermal material is likely derived from the dehydration of the Cocos Plate at greater depths, and that the upwelling channel beneath the Azul Volcano is separated in the uppermost mantle.

The anisotropy of the Pn wave in Central America shows strong NW-SE characteristics, which are parallel to the direction of the plate collision boundary and consistent with the direction of most SKS fast wave in this region. This feature has also been found in the Japanese island arc and the Lesser Antilles island arc (Lü et al., 2019, 2021). We argue that subduction dehydration caused the olivine crystals in the uppermost mantle to have a B-type structure, thus showing strong anisotropy parallel to the collision boundary (Katayama et al., 2009; Kneller et al., 2005). Another possible explanation is that the parallel anisotropy of the trenches is

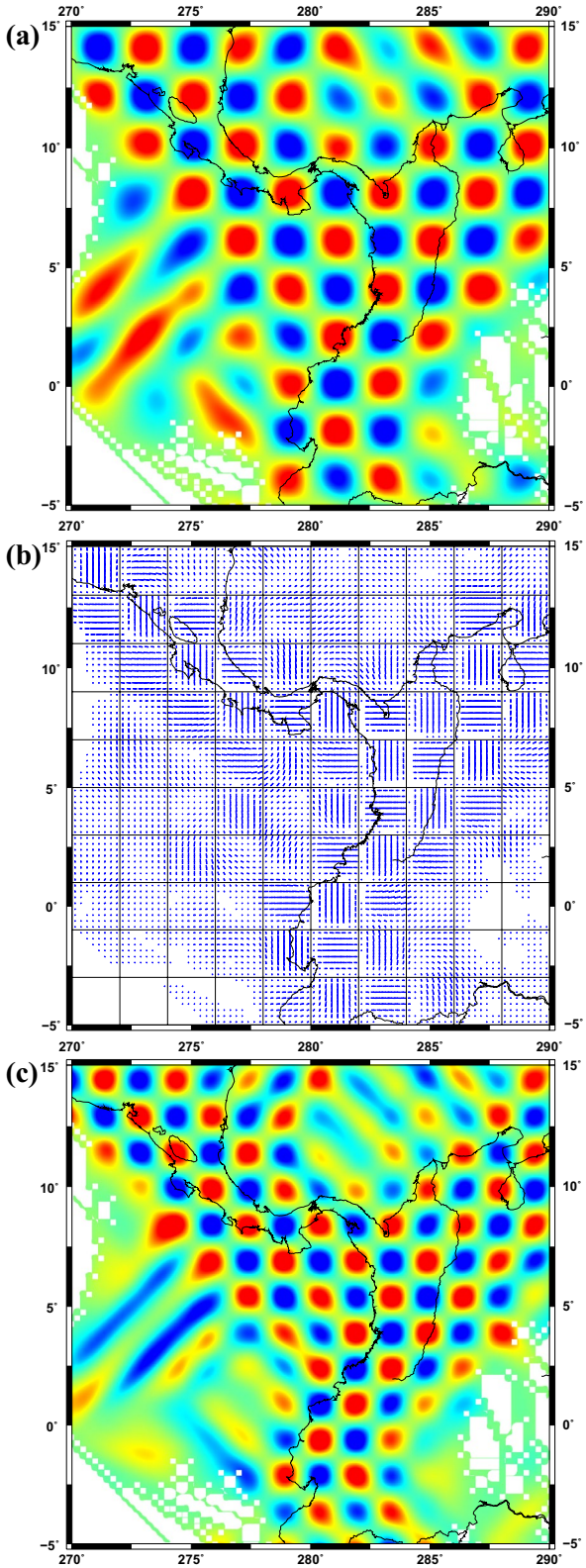

Figure 5. Checkerboard test inversion results for the (a, c) velocity and (b) anisotropy. The checkerboard sizes are (a) 2.0° × 2.0°, (b) 2.0° × 2.0°, and (c) 1.5° × 1.5°, respectively.

related to mantle flows (Abt et al., 2010; Hodges & Miller, 2015; Hoernle et al., 2008). In summary, the remarkable Pn low-velocity structure and trench-parallel anisotropy beneath the volcanic zone show the influence of plate subduction dehydration in the uppermost mantle. We believe that the strong anisotropy in the uppermost mantle dominates most SKS splitting in this region, so the direction of these SKS fast directions is consistent with that of Pn anisotropy. In addition, we observe that certain SKS measurements west of the arc belt have a fast direction parallel to the subduction direction. We suggest that these SKS splitting are more affected by the anisotropic structures at other depths, and a kind of arc-perpendicular anisotropic structure might exist and contribute to the SKS observations west of the arc belt.

4.2. Caribbean Sea-Panama-Northern Colombia

In the Caribbean region in the northern part of the study region, the uppermost mantle has mainly high velocities, indicating that the uppermost mantle in this area is stable and is less affected by the mantle thermal material caused by the subduction of the Cocos Plate. In Panama, the strong low-velocity zone in the uppermost mantle of Central America ends eastward in central Panama (~280°E). This feature outlines the eastern edge of the subducted Cocos Plate, indicating that the influence of the mantle thermal material caused by subduction ends eastward in central Panama. Our results support that eastern Panama is the plate window of the Farallon Plate (Hey, 1977; van Benthem et al., 2013). To the north of this region, there is a Benioff zone located in the northern part of the Panama microplate, indicating a southward subduction of the Caribbean Plate (Camacho et al., 2010). Meanwhile, we observed a small-scale low-velocity structure in eastern Panama: we suggest that the southward subduction of the Caribbean Plate caused some dehydration and mantle hot material upwelling.

In the northeastern part of our study area, there is a high-velocity strip beneath western Venezuela, which is consistent with the high-velocity structure observed by previous three-dimensional imaging methods and is likely the subducted ancient Caribbean Plate (Bezada et al., 2010). A weak low-velocity anomaly has been observed near 286°E in the North Andes Block, which we argue may be related to the eastward subduction of the Nazca Plate. There may be upwelling of hot material beneath this area, but it is relatively weak. The weak low-velocity structure observed near 288°E in the Maracaibo Block is connected with the low-velocity structure underneath northern South America discovered by previous study (Miller et al., 2009). This low-velocity structure may be caused by the westward movement of hot mantle material in the Lesser Antilles subduction zone (Masy et al., 2011; Miller et al., 2009). The anisotropic structure of the Pn wave in this region lacks strong characteristics; it is messy and has a low correlation with the SKS anisotropic structure. We believe that this illustrates the complex mantle structure of this area; that is, the Nazca, Farallon, and Caribbean Plates are all subducted under the South American Plate, resulting in complex seismic anisotropic structures in different regions and at different depths; thus, SKS splitting measurements, affected by a wide range of depths, have low correlation with the anisotropic structure of the uppermost mantle.

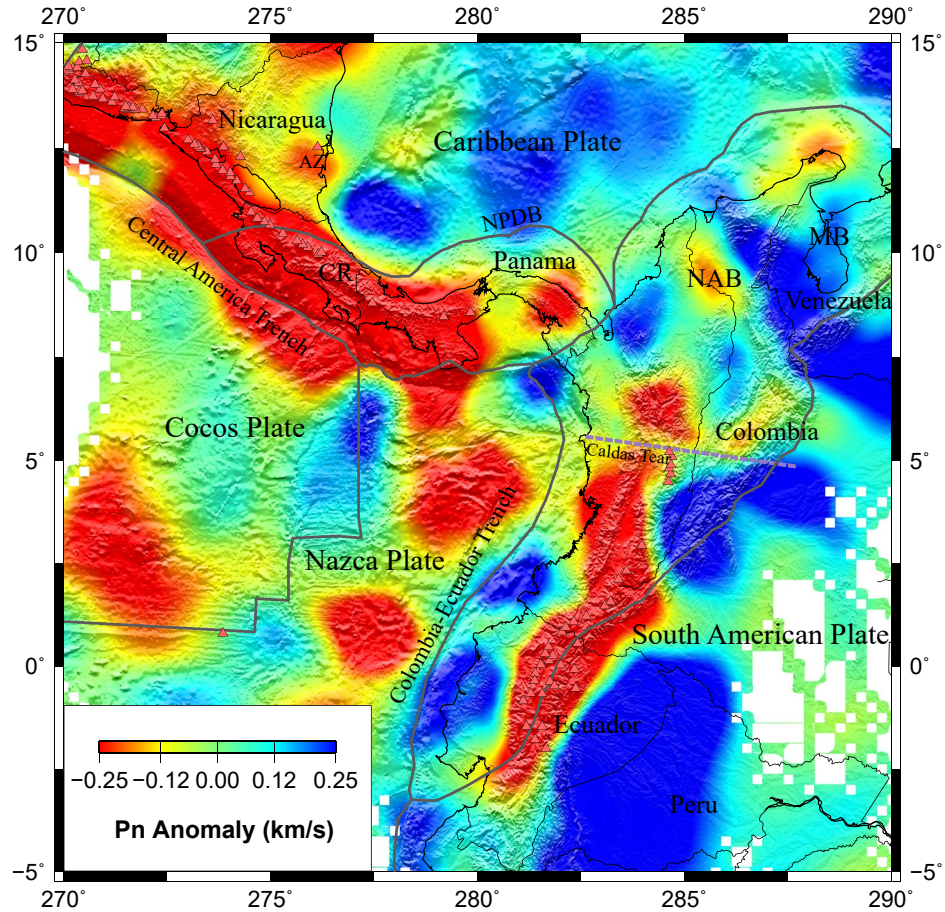

Figure 6. Pn velocity image of Central America and northwestern South America area. The colors represent the velocity differences relative to 8.0 km/s: red represents low velocities, blue represents high velocities. Triangles represent Quaternary volcanoes. Gray lines denote tectonic boundaries. AZ, Azul Volcano; CR, Costa Rica; MB, Maracaibo Block; NAB, North Andes Block; NPDB, North Panama Deformed Belt.

4.3. Western Colombia-Ecuador

In western Colombia and Ecuador, we observed a strong (low anomalies larger than 5%) north-south banded low-velocity structure in the uppermost mantle, which shows that the Nazca Plate subducted eastward below the South American Plate. We suggest that the dehydration of the subducted plate caused the high temperature or partial melting in the uppermost mantle and result to a banded distribution of volcanoes on the surface. The volcanoes near 5°N, 285°E are located to the east of the low-velocity structure of the mantle, which we think is due to the tilt and rise of thermal material from the mantle to the surface in this area. Similarly to the lower part of the Central American volcanic belt, the anisotropic structure of Pn waves below this volcanic belt is consistently parallel to the plate collision boundary, while the strength of Pn anisotropy are larger than 3%. In this region, the existing shear wave splitting structures are very complex, including a complicated pattern of SKS fast direction parallel to the plate boundary and other oblique directions (Idarraga-Garcia et al., 2016). We believe that in addition to the strong anisotropy in the uppermost mantle, the anisotropy at other depths is also strong and not parallel to the direction of the plate boundary, which makes the direction of SKS fast waves in different depth sampling ranges different. We agree with the view proposed by Idarraga-Garcia et al. (2016) that there is an anisotropic fast wave direction parallel to the subduction direction due to the mantle flow beneath the subducted plate.

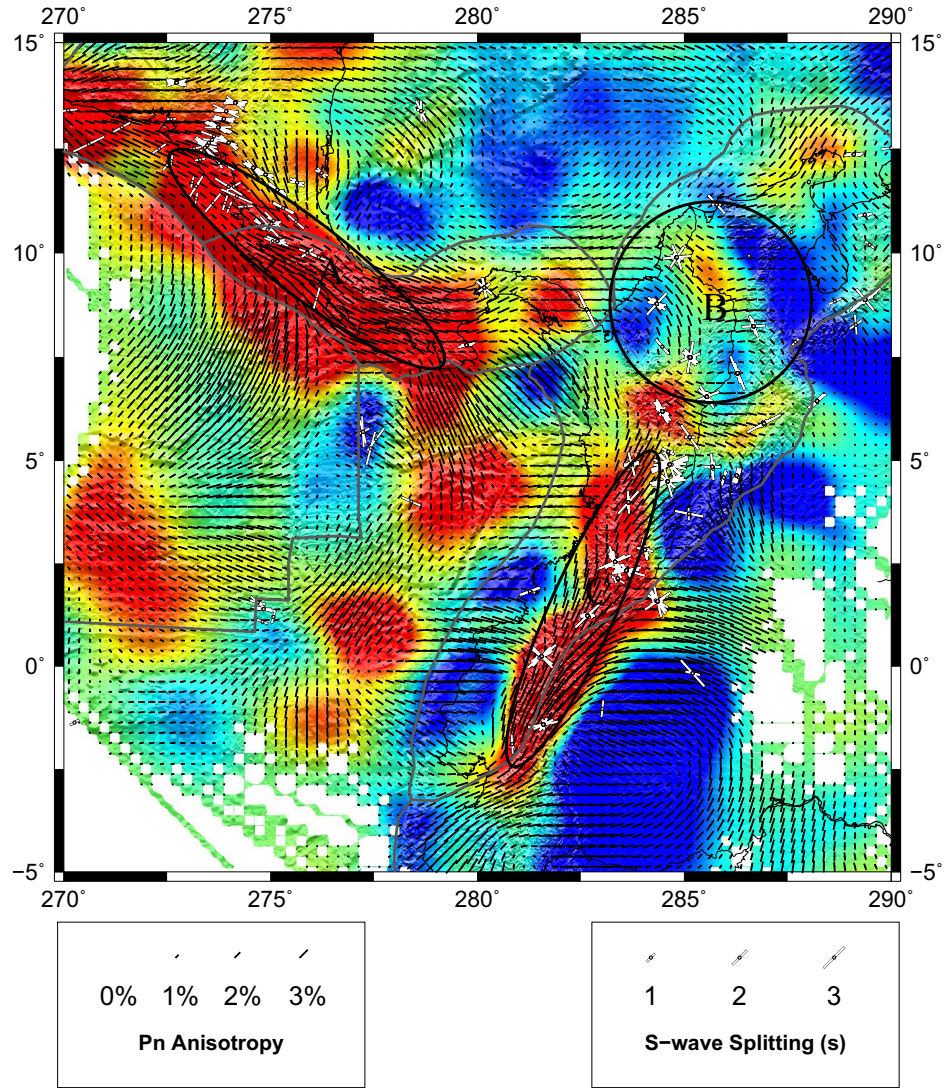

Figure 7. Pn velocity and anisotropy images of Central America and northwestern South America area. Regions with dense ray coverage and significant anisotropy patterns are outlined with black ovals. Short black bars represent the fastest Pn direction. The lengths of black bars are proportional to the magnitude of Pn anisotropy. White bars with pink core represent shear wave splitting measurements (Abt et al., 2010; Growdon et al., 2009; Idarraga-Garcia et al., 2016; Lynner & Long, 2014; Piñero-Feliciangeli & Kendall, 2008; Porritt et al., 2014; Russo & Silver, 1994).

In central Colombia, previous studies have revealed obvious differences in earthquake distribution between the north and south of the Caldas Tear Zone (Engdahl et al., 2020; Idarraga-Garcia et al., 2016). Our imaging results clearly show that there is an obvious discontinuity in the Pn velocity and anisotropic structure at the uppermost mantle on both sides of the Caldas Tear. Idarraga-Garcia et al. (2016) also found obvious changes in the direction of SKS fast waves on both sides of the tear band. These results reveal differences in the subduction direction, distance and angle between the two sides of the tearing plate, which leads to structural dislocation on the north and south sides. The Pn low-velocity discontinuity also indicates that there is less dehydration near the tear zone and that there may be a magmatic gap (Figure 8).

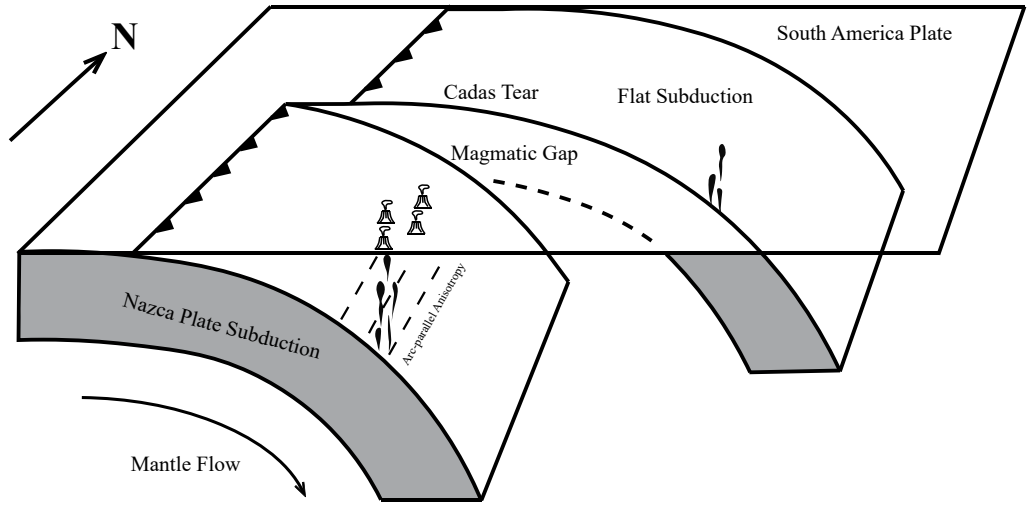

Figure 8. Diagram of the structure around the Caldas Tear Zone. There are differences in the subduction direction, distance and angle between both sides of the tearing plate. Trench-parallel anisotropy of uppermost mantle exists beneath the volcanic arc, while arc-perpendicular anisotropy due to the mantle flow exists beneath the subducted plate.

5. Conclusions

We obtained the first comprehensive and high-resolution Pn velocity and anisotropy model of the uppermost mantle in Central America and northwestern South America. Significantly low Pn velocities and arc-parallel anisotropic structures are observed beneath the volcanic arc in Central America, indicating the serious effect of Cocos Plate subduction. The separate, low Pn velocity beneath the back-arc volcano in Nicaragua shows that the hot material upwelling in the uppermost mantle beneath this volcano is separated from the main volcanic arc. High Pn velocities are observed beneath the stable Caribbean Plate. We argue that the low Pn velocity in eastern Panama is attributed to the southward subduction and dehydration of the Caribbean Plate. The high Pn velocity beneath western Venezuela is likely the subducted ancient Caribbean Plate. Low Pn velocities are also observed beneath the Colombia-Ecuador volcanic arc. Combining the Pn anisotropic structure and previous SKS measurements, we support the model that proposes strong arc-parallel anisotropy in the uppermost mantle beneath the Colombia-Ecuador volcanic arc and possible arc-perpendicular anisotropy in the deeper mantle beneath the subducted plate. The Pn velocity and anisotropic pattern are discontinuous on both sides of the Caldas Tear, and a magmatic gap may exist near the tear zone.

Data Availability Statement

The seismic data are from the website of International Seismological Centre (http://www.isc.ac.uk/isc-ehb; https://doi.org/10.31905/D808B830).

Acknowledgments
We thank the editor Prof. Michael Bostock, the associate editor and two anonymous reviewers for their helpful suggestions. The research is supported by the National Natural Science Foundation of China (Grants 41874066, 41674066) and the Key Research Program of the Institute of Geology & Geophysics, CAS (Grant IGGCAS-201904).

References

Abt, D. L., Fischer, K. M., Abers, G. A., Protti, M., Gonzalez, V., & Strauch, W. (2010). Constraints on upper mantle anisotropy surrounding the Cocos slab from SK(K)S splitting. *Journal of Geophysical Research*, *115*, B06316. https://doi.org/10.1029/2009JB006710

Amaru, M. L. (2007). *Global travel time tomography with 3-D reference models*. (Ph.D. thesis). Utrecht University, Geology Ultraiectina.

Becker, T. W., Lebedev, S., & Long, M. D. (2012). On the relationship between azimuthal anisotropy from shear wave splitting and surface wave tomography. *Journal of Geophysical Research*, *117*, B01306. https://doi.org/10.1029/2011JB008705

Bezada, M. J., Levander, A., & Schmandt, B. (2010). Subduction in the southern Caribbean: Images from finite-frequency P wave tomography. *Journal of Geophysical Research*, *115*, B12333. https://doi.org/10.1029/2010JB007682

Bijwaard, H., Spakman, W., & Engdahl, E. R. (1998). Closing the gap between regional and global travel time tomography. *Journal of Geophysical Research*, *103*, 30055–30078. https://doi.org/10.1029/98JB02467

Brasse, H., Schafer, A., Diaz, D., Alvarado, G. E., Munoz, A., & Mütschard, L. (2015). Deep-crustal magma reservoirs beneath the Nicaraguan volcanic arc, revealed by 2-D and semi 3-D inversion of magnetotelluric data. *Physics of the Earth and Planetary Interiors*, *248*, 55–62. https://doi.org/10.1016/j.pepi.2015.08.004

Buehler, J. S., & Shearer, P. M. (2010). Pn tomography of the Western United States using USArray. *Journal of Geophysical Research*, *115*, B09315. https://doi.org/10.1029/2009JB006874

Buehler, J. S., & Shearer, P. M. (2017). Uppermost mantle seismic velocity structure beneath USArray. *Journal of Geophysical Research: Solid Earth*, *122*, 436–448. https://doi.org/10.1002/2016JB013265

Camacho, E., Hutton, W., & Pacheco, J. F. (2010). A new look at evidence for a Wadati-Benioff zone and active convergence at the north Panama deformed belt. *Bulletin of the Seismological Society of America*, *100*(1), 343–348. https://doi.org/10.1785/0120090204

Carr, M. J., Feigenson, M. D., Patino, L. C., & Walker, J. A. (2003). Volcanism and geochemistry in central America: Progress and problems. In: Inside the subduction Factory. In J.Eiler (Ed.), *Geophysical Monograph Series*(Vol. 138, pp. 153–174). AGU. https://doi.org/10.1029/138gm09

Engdahl, E. R., Giacomo, D. D., Sakarya, B., Gkarlaouni, C. G., Harris, J., & Storchak, D. A. (2020). ISC-EHB 1964–2016, an improved data set for studies of Earth structure and global seismicity. *Earth and Space Science*, *7*, e2019EA000897. https://doi.org/10.1029/2019EA000897

Fan, X., Chen, Q.-F., Ai, Y., Chen, L., Jiang, M., Wu, Q., & Guo, Z. (2021). Quaternary sodic and potassic intraplate volcanism in northeast China controlled by the underlying heterogeneous lithospheric structures. *Geology*, *49*(10), 1260–1264. https://doi.org/10.1130/G48932.1

Growdon, M. A., Pavlis, G. L., Niu, F., Vernon, F. L., & Rendon, H. (2009). Constraints on mantle flow at the Caribbean–South American plate boundary inferred from shear wave splitting. *Journal of Geophysical Research*, *114*, B02303. https://doi.org/10.1029/2008JB005887

Harmon, N., Cruz, M., Rychert, C., Abers, G., & Fischer, K. (2013). Crustal and mantle shear velocity structure of Costa Rica and Nicaragua from ambient noise and teleseismic Rayleigh wave tomography. *Geophysical Journal International*, *195*, 1300–1313. https://doi.org/10.1093/gji/ggt309

Harris, C. W., Miller, M. S., & Porritt, R. W. (2018). Tomographic imaging of slab segmentation and deformation in the Greater Antilles. *Geochemistry, Geophysics, Geosystems*, *19*, 2292–2307. https://doi.org/10.1029/2018GC007603

He, Y., & Lü, Y. (2021). Anisotropic Pn tomography of Alaska and adjacent regions. *Journal of Geophysical Research: Solid Earth*, *126*, e2021JB022220. https://doi.org/10.1029/2021JB022220

Hearn, T. M. (1996). Anisotropic Pn tomography in the Western United States. *Journal of Geophysical Research*, *101*(B4), 8403–8414. https://doi.org/10.1029/96JB00114

Hearn, T. M. (1999). Uppermost mantle velocities and anisotropy beneath Europe. *Journal of Geophysical Research*, *104*(B7), 15123–15139. https://doi.org/10.1029/1998JB900088

Hearn, T. M., & Ni, J. (1994). Pn velocities beneath continental collision zones: The Turkish-Iranian plateau. *Geophysical Journal International*, *117*, 273–283. https://doi.org/10.1111/j.1365-246X.1994.tb03931.x

Hey, R. (1977). Tectonic evolution of the Cocos-Nazca spreading center. *The Geological Society of America Bulletin*, *88*, 1404–1420. https://doi.org/10.1130/0016-7606(1977)88<1404:TEOTCS>2.0.CO;2

Hodges, M., & Miller, M. S. (2015). Mantle flow at the highly arcuate northeast corner of the Lesser Antilles subduction zone: Constraints from shear-wave splitting analyses. *Lithosphere*, *7*(5), 579–587. https://doi.org/10.1130/L440.1

Hoernle, K., Abt, D. L., Fischer, K. M., Nichols, H., Hauff, F., Abers, G. A., et al. (2008). Arc-parallel flow in the mantle wedge beneath Costa Rica and Nicaragua. *Nature*, *451*, 1094–1097. https://doi.org/10.1038/nature06550

Idarraga-Garcia, J., Kendall, J.-M., & Vargas, C. A. (2016). Shear wave anisotropy in northwestern South America and its link to the Caribbean and Nazca subduction geodynamics. *Geochemistry, Geophysics, Geosystems*, *17*, 3655–3673. https://doi.org/10.1002/2016GC006323

Karato, S., & Jung, H. (1998). Water, partial melting and the origin of the seismic low velocity and high attenuation zone in the upper mantle. *Earth and Planetary Science Letters*, *157*(3–4), 193–207. https://doi.org/10.1016/s0012-821x(98)00034-x

Katayama, I., Hirauchi, K. I., Michibayashi, K., & Ando, J. I. (2009). Trench-parallel anisotropy produced by serpentine deformation in the hydrated mantle wedge. *Nature*, *461*(7267), 1114–1117. https://doi.org/10.1038/nature08513

Kneller, E. A., Van Keken, P. E., Karato, S. I., & Park, J. (2005). B-type olivine fabric in the mantle wedge: Insights from high-resolution non-Newtonian subduction zone models. *Earth and Planetary Science Letters*, *237*(3), 781–797. https://doi.org/10.1016/j.epsl.2005.06.049

Lei, J., Li, Y., Xie, F., Teng, J., Zhang, G., Sun, C., & Zha, X. (2014). Pn anisotropic tomography and dynamics under eastern Tibetan plateau. *Journal of Geophysical Research: Solid Earth*, *119*, 2174–2198. https://doi.org/10.1002/2013JB010847

Li, C., van der Hilst, R. D., Engdahl, E. R., & Burdick, S. (2008). A new global model for P wave speed variations in Earth's mantle. *Geochemistry, Geophysics, Geosystems*, *9*, Q05018. https://doi.org/10.1029/2007GC001806

Li, J., & Song, X. (2018). Tearing of Indian mantle lithosphere from high-resolution seismic images and its implications for lithosphere coupling in southern Tibet. *Proceedings of the National Academy of Sciences of the United States of America*, *115*(33), 8296–8300. https://doi.org/10.1073/pnas.1717258115

Liang, C., Song, X., & Huang, J. (2004). Tomographic inversion of Pn travel times in China. *Journal of Geophysical Research*, *109*, B11304. https://doi.org/10.1029/2003JB002789

Long, M. D., & Becker, T. W. (2010). Mantle dynamics and seismic anisotropy. *Earth and Planetary Science Letters*, *297*, 341–354. https://doi.org/10.1016/j.epsl.2010.06.036

Lonsdale, P. (2005). Creation of the Cocos and Nazca plates by fission of the Farallon Plate. *Tectonophysics*, *404*(3–4), 237–264. https://doi.org/10.1016/j.tecto.2005.05.011

Lü, Y., Li, J., Liu, L., & Zhao, L.-F. (2019). Complex uppermost mantle structure and deformation beneath the Northwest Pacific region. *Journal of Geophysical Research: Solid Earth*, *124*, 6866–6879. https://doi.org/10.1029/2019JB017356

Lü, Y., Liu, J., He, Y., & Guan, Y. (2021). New uppermost mantle Pn velocity and anisotropy model of the eastern Caribbean. *Journal of Geophysical Research: Solid Earth*, *126*, e2020JB021523. https://doi.org/10.1029/2020JB021523

Lü, Y., Ni, S., Chen, L., & Chen, Q.-F. (2017). Pn tomography with Moho depth correction from eastern Europe to Western China. *Journal of Geophysical Research: Solid Earth*, *122*, 1284–1301. https://doi.org/10.1002/2016JB013052

Lynner, C., & Long, M. D. (2014). Sub-slab anisotropy beneath the Sumatra and circum-Pacific subduction zones from source-side shear wave splitting observations. *Geochemistry, Geophysics, Geosystems*, *15*, 2262–2281. https://doi.org/10.1002/2014GC005239

Masy, J., Niu, F., Levander, A., & Schmitz, M. (2011). Mantle flow beneath northwestern Venezuela: Seismic evidence for a deep origin of the Mérida Andes. *Earth and Planetary Science Letters*, *305*(3–4), 396–404. https://doi.org/10.1016/j.epsl.2011.03.024

Menke, W. (2015). Equivalent heterogeneity analysis as a tool for understanding the resolving power of anisotropic travel-time tomography. *Bulletin of the Seismological Society of America*, *105*(2A), 719–733. https://doi.org/10.1785/0120140150

Miller, M. S., Levander, A., Niu, F., & Li, A. (2009). Upper mantle structure beneath the Caribbean-South American plate boundary from surface wave tomography. *Journal of Geophysical Research*, *114*, B01312. https://doi.org/10.1029/2007JB005507

Paige, C., & Saunders, M. (1982). Lsqr: An algorithm for sparse linear equations and sparse least squares. *ACM Transactions on Mathematical Software*, *8*(1), 43–71. https://doi.org/10.1145/355984.355989

Pei, S., Sun, Y., & Toksöz, M. N. (2011). Tomographic Pn and Sn velocity beneath the continental collision zone from Alps to Himalaya. *Journal of Geophysical Research*, *116*, B10311. https://doi.org/10.1029/2010JB007845

Pei, S., Zhao, J., Sun, Y., Xu, Z., Wang, S., Liu, H., et al. (2007). Upper mantle seismic velocities and anisotropy in China determined through Pn and Sn tomography. *Journal of Geophysical Research*, *112*, B05312. https://doi.org/10.1029/2006JB004409

Pennington, W. D. (1981). Subduction of the eastern Panama Basin and seismotectonics of northwestern South America. *Journal of Geophysical Research*, *86*(B11), 10753–10770. https://doi.org/10.1029/JB086iB11p10753

Piñero-Feliciangeli, L., & Kendall, J. M. (2008). Sub-slab mantle flow parallel to the Caribbean Plate boundaries: Inferences from SKS splitting. *Tectonophysics*, *462*, 22–34. https://doi.org/10.1016/j.tecto.2008.01.022

Porritt, R. W., Becker, T. W., & Monsalve, G. (2014). Seismic anisotropy and slab dynamics from SKS splitting recorded in Colombia. *Geophysical Research Letters*, *41*, 8775–8783. https://doi.org/10.1002/2014GL061958

Russo, R. M., & Silver, P. G. (1994). Trench-parallel flow beneath the Nazca plate from seismic anisotropy. *Science*, *263*, 1105–1111. https://doi.org/10.1126/science.263.5150.1105

Sandvol, E. A., Ni, J. F., Hearn, T. M., & Roecker, S. (1994). Seismic azimuthal anisotropy beneath the Pakistan Himalayas. *Geophysical Research Letters*, *21*(15), 1635–1638. https://doi.org/10.1029/94GL01386

Syracuse, E. M., Abers, G. A., Fischer, K., MacKenzie, L., Rychert, C., Protti, M., et al. (2008). Seismic tomography and earthquake locations in the Nicaraguan and Costa Rican upper mantle. *Geochemistry, Geophysics, Geosystems*, *9*, Q07S08. https://doi.org/10.1029/2008GC001963

Taboada, A., Rivera, L., Fuenzalida, A., Cisternas, A., Philip, H., Bijwaard, H., et al. (2000). Geodynamics of the northern Andes: Subductions and intracontinental deformation (Colombia). *Tectonics*, *19*, 787–813. https://doi.org/10.1029/2000TC900004

Van Avendonk, H. J. A., Holbrook, W. S., Lizarralde, D., & Denyer, P. (2011). Structure and serpentinization of the subducting Cocos plate offshore Nicaragua and Costa Rica. *Geochemistry, Geophysics, Geosystems*, *12*, Q06009. https://doi.org/10.1029/2011GC003592

van Benthem, S., Govers, R., Spakman, W., & Wortel, R. (2013). Tectonic evolution and mantle structure of the Caribbean. *Journal of Geophysical Research: Solid Earth*, *118*, 3019–3036. https://doi.org/10.1002/jgrb.50235

van der Hilst, R. D., Widiyantoro, S., & Engdahl, E. R. (1997). Evidence for deep mantle circulation from global tomography. *Nature*, *386*, 578–584. https://doi.org/10.1038/386578a0

Vargas, C. A., & Mann, P. (2013). Tearing and breaking off of subducted slabs as the result of collision of the Panama Arc-indenter with northwestern South America. *Bulletin of the Seismological Society of America*, *103*(3), 2025–2046. https://doi.org/10.1785/0120120328

Zhao, D., Yu, S., & Liu, X. (2016). Seismic anisotropy tomography: New insight into subduction dynamics. *Gondwana Research*, *33*, 24–43. https://doi.org/10.1016/j.gr.2015.05.008